Biogeochemistry (2025) 168:58
https://doi.org/10.1007/s10533-025-01248-1

The role of different exogenous NO concentrations on C and N biogeochemistry of an agricultural soil

Logapragasan Subramaniam · Eduardo Perez-Valera · Antoine Berger · Ulrike Ostler · Florian Engelsberger · Nicolas Brüggemann · Laurent Philippot · Klaus Butterbach-Bahl · Michael Dannenmann

Received: 1 February 2025 / Accepted: 18 June 2025 / Published online: 16 July 2025

Abstract The signaling compound nitric oxide (NO) might play an important, yet unquantified role in mediating soil biogeochemical Carbon and Nitrogen cycles. This study quantified the effects of different soil-typical exogenous NO concentrations on the microbial community, on fertilizer N turnover, and on C and N trace gas fluxes of agricultural soil. For this, we repeatedly established soil NO concentrations of either 0, 200, 400, and ppbv-NO in soil mesocosms for in total of 12 days, followed by high-resolution automated measurements of CO_2, NO, CH_4, and N_2O fluxes, molecular analysis of microbial community composition and ^{15}N-isotope-tracing based assessment of fertilizer N turnover. We found no effects of different NO levels on microbial communities and CO_2, CH_4, and NO fluxes. However, at 200 ppbv concentration, exogenous NO promoted microbial assimilation of fertilizer N. In contrast, at 400 ppbv-NO concentration, microbial biomass N was reduced, and microbial uptake of fertilizer N was inhibited, accompanied by a 33% reduction of N_2O emissions. This suggested a promoting effect of 200 ppbv-NO on the physiology of cells involved in heterotrophic microbial N turnover, probably reinforcing the role of cell-endogenous NO. In contrast, the higher exogenous NO concentrations of 400 ppbv seemed to inhibit heterotrophic microbial inorganic N assimilation, with however no increase in N_2O emissions due to detoxification mechanisms. In conclusion, our pioneering study provides first insights into impacts of exogenous NO on soil C and N biogeochemistry in

Logapragasan Subramaniam and Eduardo Perez-Valera have contributed equally to this work.

Responsible Editor: Marie-Anne de Graaff.

Supplementary Information The online version contains supplementary material available at https://doi.org/10.1007/s10533-025-01248-1.

L. Subramaniam · U. Ostler · F. Engelsberger · K. Butterbach-Bahl · M. Dannenmann (✉)
Institute for Meteorology and Climate Research Atmospheric Environmental Research (IMKIFU), Division "Terrestrial Bio-Geo-Chemistry", Karlsruhe Institute of Technology (KIT), KIT Campus Alpin, Kreuzeckbahnstr. 19, 82467 Garmisch-Partenkirchen, Germany
e-mail: michael.dannenmann@kit.edu

E. Perez-Valera · A. Berger
Univ Bourgogne, INRAE, Institut Agro Dijon, Agroecologie, 17 Rue Sully, 21000 Dijon, France

N. Brüggemann · L. Philippot
Institute of Bio-and Geosciences, Agrosphere (IBG-3), Forschungszentrum Jülich GmbH, 52428 Jülich, Germany

K. Butterbach-Bahl
Center for Landscape Research in Sustainable Agricultural Futures - Land-CRAFT, Department of Agroecology, Aarhus University, Ole Worms Allé 3, 8000 Aarhus C, Denmark

natural soil systems and reveals a NO concentration-dependent regulation of microbial N retention.

Keywords Automated mesocosm system · Nitric oxide (NO) · Soil gas fluxes · Microbial activity

Introduction

Nitric oxide (NO) is a colorless, odorless gas with significant effects on human health and key roles in plant and soil microbial metabolism (Fowler et al. 2009). As a reactive free radical, NO is a primary nitrogen (N) oxide, that is produced and consumed by microbial activity, soil physico-chemical reactions, combustion processes, and plant physiological pathways (Medinets et al. 2015; Olivier et al. 1998; Wendehenne et al. 2014). In plants, NO acts as a critical signaling molecule, regulating growth, development (e.g., seed germination, root growth, stomatal closure), and responses to biotic (e.g., pathogens, parasites) and abiotic (e.g., drought, salinity) stresses (Gupta et al. 2022; Ma et al. 2020; Wendehenne et al. 2014; Yu et al. 2014). Nitric oxide also plays a multifaceted role in soil microbial physiology, e.g., serving as an essential intermediate in N metabolism, as a signaling compound essential for cell physiology, and as a toxic molecule, requiring bacterial regulatory and protective mechanisms (Rinaldo et al. 2018). Due to its free diffusivity across biological membranes, both cell-endogenous and cell-exogenous NO can modulate the activities of cellular and extracellular proteins, thereby implementing important physiological functions (Medinets et al. 2015).

In well-aerated soils, autotrophic bacteria such as *Nitrosobacteria* and *Nitrobacteria* as well as ammonia-oxidizing archaea (AOA) produce NO as a by-product during the oxidation of ammonium (NH_4^+) to hydroxylamine (NH_2OH) in nitrification, before its subsequent conversion to nitrite (NO_2^-) and nitrate (NO_3^-), utilizing oxygen (O_2) as the electron acceptor (Conrad 1996; Butterbach-Bahl 2011), High gas diffusivity allows NO to escape into soil or further to the atmosphere before further reduction (Heil et al. 2016; Skiba et al. 1997). In addition, NO serves as an intermediate in nitrifier-denitrification, a process facilitated by ammonia-oxidizing bacteria (AOB), such as *Nitrosomonas europaea*, and AOA, such as *Nitrosopumilus maritimus*. Under O_2-limited conditions, NO produced during ammonia oxidation is detoxified into nitrous oxide (N_2O) or dinitrogen (N_2) (Martens-Habbena et al. 2015; Remde and Conrad 1990; Wrage et al. 2001).

In soils with higher water-filled pore space (WFPS), many anaerobic microsites allow for denitrification (Groffman et al. 2006). This process is facilitated by a series of metalloenzymes, including nitrate reductase (Nar and Nap), nitrite reductase (Nir), nitric oxide reductase (Nor), and nitrous oxide reductase (Nos). Nitric oxide is a free and obligatory intermediate produced by nitrite reductases and is subsequently reduced to N_2O and N_2 (Borrero-de Acuña et al. 2016). Two primary nitrite reductases-cytochrome cd_1, commonly found in Gram-negative bacteria, and copper-containing nitrite reductase, catalyze the production of NO (Korner and Zumft 1989; Jackson et al. 1991). Genetic studies in *Pseudomonas aeruginosa* have identified nitric oxide reductase (NorBC) and the regulatory protein NosR as essential components of the denitrification network, with NorBC facilitating NO reduction to N_2O and NosR regulating Nos gene expression and machinery assembly (Borrero-de Acuña et al. 2016 and 2017). In addition, Nor, a membrane-bound enzyme located in the periplasmic space, converts NO to N_2O, maintaining low intracellular NO levels (1–30 nM) in bacteria like *Pseudomonas stutzeri* and *Azospirillum brasilense*, thereby protecting cells from NO-induced damage (Remde and Conrad 1991). The activity of Nir and Nor varies with the bacterial species as well as environmental factors like pH, O_2 levels, and substrate availability (Bergaust et al. 2010; De Boer et al. 1996; Ray and Spiro 2023). Additionally, NO inhibits key microbial enzymes by forming nitrosyl complexes: nitrogenase, critical for nitrogen fixation (e.g., rhizobia–legume symbiosis); cytochrome aa_3 in heme-copper oxidases, which affects O_2 reduction, and Nor, which interferes with the conversion of NO to N_2O (Hayashi et al. 2007; Hendriks et al. 1998; Sánchez et al. 2011). These processes are integral to N cycling and play a crucial role in bacterial energy conservation. The reduction of NO to N_2O is coupled with proton translocation in some species, enabling ATP synthesis under O_2-limited conditions (Gopalasingam et al. 2019).

Beyond the soil biological process, NO undergoes both non-enzymatic and chemical transformations in soil, contributing to its detoxification and the N cycle.

It reacts with reduced metals like Fe^{2+} and organic matter, forming intermediates such as hyponitrite ($N_2O_2^{2-}$) and resulting in the production of N_2O or N_2 (Jones et al. 2015; Lionetti et al. 2016). Additionally, NO interacts with oxidized soil components, such as manganese oxides, facilitating its oxidation to NO_3^- (Zhang et al. 2018). Furthermore, NO exhibits significant toxicity to bacteria through the formation of reactive species like peroxynitrite ($ONOO^-$), which oxidizes sulfhydryl groups in proteins, impairing their functionality (Ji et al. 2006). Additionally, NO interacts with proteins to form S-nitrosothiols and causes DNA damage via cytosine deamination, resulting in mutagenic effects, such as C → T transitions (Smith and Marletta 2012; Wink et al. 1991). In fungi, NO induces nitrosative stress, disrupts cellular structures, and impairs critical processes like growth and virulence, as observed in *Candida albicans* and *Aspergillus nidulans* (Amahisa et al. 2024; Chiranand et al. 2008). To counteract these toxic effects, protective strategies include NO-binding cytochrome c′, which mitigates NO toxicity by acting as a storage or detoxification mechanism (Mayburd and Kassner 2002), while reversible S-nitrosation regulates protein activity and protective gene expression, enabling bacteria to adapt to nitrosative stress (Gusarov and Nudler 2012). These enzymatic activities are tightly regulated at transcriptional and post-transcriptional levels, allowing bacteria to efficiently balance N metabolism while minimizing the accumulation of toxic NO intermediates. The transient presence of NO is regulated by Nor, which facilitates efficient N metabolism while mitigating toxicity, thereby enabling bacteria to thrive across diverse ecological niches (Hino et al. 2010). Moreover, maintaining an optimal NO balance is critical; elevated concentrations promote biofilm formation (e.g., *Pseudomonas aeruginosa*), whereas reduced levels enhance bacterial motility (Fuente-Núñez et al. 2013).

Despite these multiple effects of NO and interactions of NO with microorganisms as revealed in pure culture and molecular studies, the actual quantitative role of different exogenous NO concentrations on biogeochemical C and N turnover processes and trace gas production under natural soil conditions is largely unknown. Nevertheless, most previous studies on microbial resilience to exogenous NO have focused on clinical settings (Ghaffari et al 2006; Miller et al. 2004 and 2009). Here we conducted a pioneering study to address the key knowledge gap on how different NO concentrations affect soil microbial community, biogeochemical C and N turnover, and soil-atmosphere exchange of C and N trace gases in agricultural soil. To achieve this, we utilized a recently developed automated soil mesocosm system, that allows precise manipulation of soil and headspace NO concentrations while continuously monitoring C and N trace gas fluxes (Subramaniam et al. 2024). In this study, we used this system to manipulate soil NO concentrations in combination with the application of ^{15}N labeled mineral fertilizer to quantify fertilizer N turnover and fate, and C and N trace gas fluxes as influenced by different NO levels. The NO exposure levels were chosen based on long-term high resolution soil air NO concentration measurements in a N-saturated temperate forest soil (Medinets et al. 2019).

We hypothesized that exogenous NO would significantly alter the microbial community and, thus, mineral N turnover and microbial N assimilation, as well as N and C trace gas exchange between the soil and atmosphere. Specifically, we expected that high NO concentrations (400 ppbv) would negatively soil respiration and microbial N uptake due to their toxicity. However, detoxification at these concentrations would likely increase N_2O emissions, whereas such effects would not be observed at more moderate NO concentrations (200 ppbv).

Materials and methods

Soil preparation for incubation

The soil used throughout the experiment was obtained from abandoned cropland at CEREEP (Centre de Recherche en Ecologie Prédictive) situated in Saint-Pierre-les-Nemours, France (48°17′14.48″ N, 2°40′34.64″ E). We chose the soil because it is representative for many agricultural soils in central Europe and provides good diffusive properties. The soil is classified as Cambisol (IUSS Working Group WRB 2022) and has a sandy loam texture, consisting of 74.1% sand (0.02–2 mm), 19% silt (0.002–0.02 mm), and 6.9% clay (< 0.002 mm). Other soil characteristics include a soil organic carbon content of 14.7 g kg^{-1}, a total nitrogen content of 1.19 g kg^{-1}, and an average bulk density of 1.3 kg m^{-3}. The initial

soil pH was 7.73. After collection, the soil was sieved at 4 mm, homogenized, air-dryed, and stored at 4 °C to limit microbial activity until the start of the experiment. The soil was then packed into the cylindrical incubation mesocosms (see below) of the incubation system. This process involved layering the soil material in 2 cm increments, thereby compressing it to attain the original bulk density of 1.3 g cm^{-3}, to a final height of 10 cm (1633 g soil dry weight per mesocosm).

Automated soil mesocosm incubation system

The study used an automated soil mesocosm incubation system consisting of a thermostatic cabinet, incubation vessels, a control unit, a NO mixing device, and a multi-gas analyzer to perform incubations under controlled conditions and to measure C and N gas concentrations at high resolution after adjusting soil NO levels (Subramaniam et al. 2024). As illustrated in (Fig. 1), the system housed twelve cylindrical soil mesocosms (internal Ø: 126.5 mm, inner height: 200 mm, volume: 2512 cm^3) made of polymethyl methacrylate, which were divided into two blocks for each experimental iteration. The first block, referred to as untreated, contained six mesocosms exposed only to ambient air without NO [NO_0]. The second block, referred to as treated, was exposed to elevated NO concentrations (Experiment 1: 200 ppbv–NO [NO_{200}] and Experiment 2: 400 ppbv–NO [NO_{400}]) by mixing NO with synthetic air in an additional gas mass flow controller to achieve the predefined levels. To ensure gas tightness, the mesocosms were equipped with double-sealed lids. Airflow for flushing the mesocosms could be controlled and directed by mass flow controllers and solenoid valves from either the headspace or the bottom. A computerized control unit allowed control of temperature, humidity, headspace, and soil gas flow. Gas flow from the mesocosms was directed through multi-position valves to a multi-gas analyzer for continuous monitoring of trace gas concentrations, including NO, N_2O, NO_2, CH_4, and CO_2, using mid-infrared laser spectrometry under

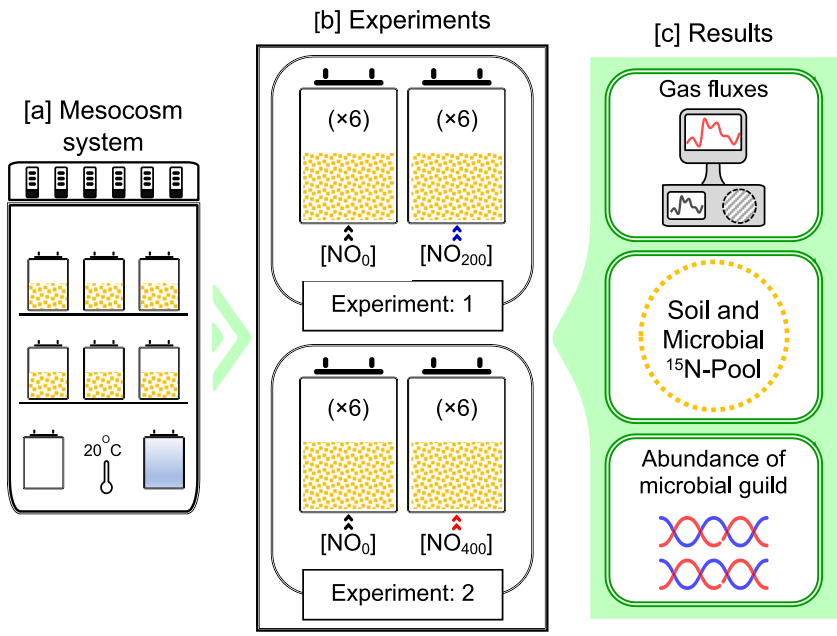

Fig. 1 Scheme of the experimental incubation and measurements. This figure showcases the soil mesocosm incubation system, which includes a bottom inlet for soil flushing with NO. Panel **a** presents the setup of the soil-incubation system, while panel **b** illustrates the plant-free soil experiment comparing control mesocosms, which received NO-free air [NO_0], to those treated with nitric oxide-enhanced air at concentrations of 200 ppbv-NO [NO_{200}] in Experiment 1 and 400 ppbv-NO [NO_{400}] in Experiment 2, with each treatment block containing six replicates and panel [c] shows the experimental outcomes, including continuous gas flux measurements, microbial N turnover, and microbial guild analysis

vacuum conditions. This process followed a 144-min sampling sequence, consisting of a 6-min measurement for each mesocosm (outlet) and a 6-min measurement for the reference chamber (inlet) across the 12 mesocosms. The entire system was operated in either the NO soil flush mode or in the headspace gas flux measurement mode. That was, during the incubation we repeatedly established periods of soil NO flushing followed by periods of trace gas flux measurement (Fig. 2). The collected data were analyzed by a custom R-package to calculate trace gas fluxes, using average gas concentrations during steady-state conditions to quantify soil mesocosm gas exchange, based on the mass balance of inlet and outlet concentrations. Further technical details on the system and the calculation of trace gas flux rates can be found in (Subramaniam et al. 2024).

Soil incubation condition and NO treatment application

We performed two consecutive incubation experiments of 37 days each under completely identical conditions except for the NO concentrations (soil concentrations of NO_{200} vs. NO_{400} in the treated mesocosms) (Fig. 2). Incubations started with a 6-day preincubation period at a constant temperature of 20 °C. On day 1, the WFPS of the air-dried soil was set at 20% (128 ml per mesocosm) and then adjusted to 40% WFPS (256 ml per mesocosm) starting on day 2, and was maintained at this level for the remainder of the experiment. To ensure uniform

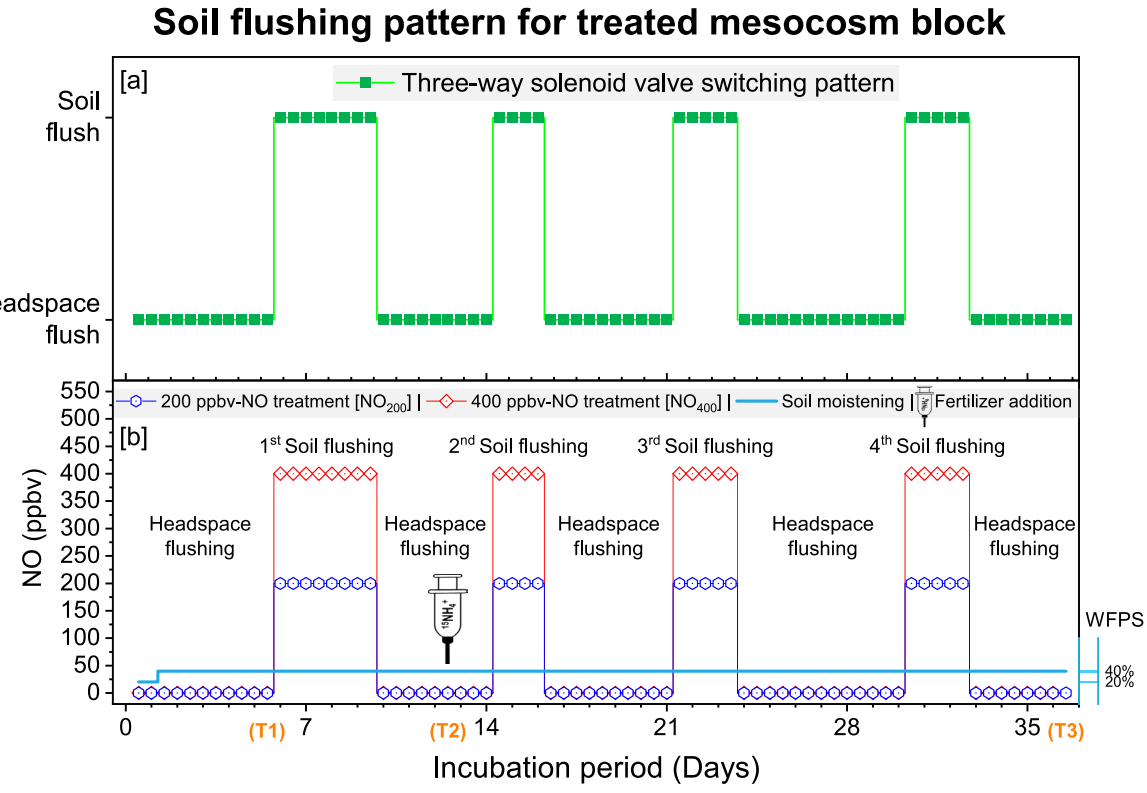

Fig. 2 Schematic representation of experimental incubation conditions for NO-treated mesocosms. The study consisted of two subsequent incubation experiments under identical conditions except for different NO concentrations in the treated mesocosms. Panel **a** illustrates the flushing pattern during alternating operations between headspace flushing (allowing for trace gas flux measurements) and soil flushing (allowing to establish soil NO concentrations of 200 or 400 ppbv), while Panel **b** represents the soil flushing patterns for treatments of Experiment 1: 200 ppbv-NO [NO_{200}] and Experiment 2: 400 ppbv-NO [NO_{400}], respectively. Both untreated and treated mesocosms were randomly arranged within the thermostatic cabinet. As indicated the soil sampling was conducted at T1 (Day 6), T2 (Day 13), and T3 (Day 37)

percolation throughout the soil column, the soil surface was sprayed several times with Milli-Q water (Subramaniam et al. 2024), with periodic adjustments made by adding Milli-Q water to maintain the desired gravimetric water content. Weeds were periodically removed from the mesocosms with sterile forceps as soon as they appeared prior to rewetting. On day 13, the soil was labeled with ($^{15}NH_4)_2SO_4$) with a 30 atomic% ^{15}N enrichment, applied at a rate of 60 kg N ha^{-1} (23.1 mg N per mesocosm) immediately after the initial NO treatment. For this purpose, 12 ml of $(^{15}NH_4)_2SO_4$ solution was injected into each mesocosm (six injections per mesocosm) at a depth of 2 cm in all twelve mesocosms using custom-made stainless steel side-port cannulas to ensure homogeneous isotope distribution and minimize immediate NH_4^+ volatilization.

Mesocosm sampling and soil biogeochemical analyses

Soil samples were taken on days 6 (T1), 13 (T2), and 37 (T3) as shown in (Fig. 2). At T1 and T2, surface soil subsamples (ca. 0–2 cm) were collected to analyze dissolved organic nitrogen (DON), NH_4^+, NO_3^-, and soil microbial biomass nitrogen (MBN) concentrations, as well as microbial community composition. Net nitrification rates were calculated from the nitrate concentration changes over time. The final sampling T3 was a complete destructive sampling of two soil layers (0–5 cm and 5–10 cm) with the primary goal of establishing the fertilizer ^{15}N balance, i.e., to analyze ^{15}N recovery in bulk soil total nitrogen (TN), extractable organic and mineral N, and microbial biomass N (Dannenmann et al. 2016). For this purpose, all soil samples were thoroughly mixed, and representative subsamples of 50 g were extracted with 0.5 M K_2SO_4 at a soil: solution ratio of 1:2 as described in detail in (Dannenmann et al. 2009). The extracts were frozen until further analysis. Subsamples of the extracts were used for the analysis of NH_4^+ and NO_3^- concentrations using a microplate spectrophotometer (Dannenmann et al. 2018), total dissolved nitrogen (TDN) and dissolved organic carbon (DOC) concentrations using a TOC/TN analyzer (Dannenmann et al. 2016). DON was calculated by subtracting mineral N concentrations from TDN concentrations (Dannenmann et al. 2016). Additional soil subsamples were extracted after chloroform fumigation, followed by TDN analysis to calculate microbial biomass using the chloroform fumigation extraction method without correction factor (Dannenmann et al. 2018). Soil extracts were also analyzed for ^{15}N enrichment in NH_4^+, NO_3^-, DON, and MBN using sequential diffusion on acid traps, followed by coupled elemental analysis-isotope ratio mass spectrometry (EA-IRMS) according to (Dannenmann et al. 2016). Approximately 10 g of soil from each depth was dried to constant weight at 55 °C, ground, and analyzed for ^{15}N content using EA-IRMS according to (Dannenmann et al. 2018). We calculated the ^{15}N excess recovery in the measured N compounds and established the fertilizer ^{15}N balance and net nitrification using the formulas provided by (Dannenmann et al. 2016).

Community composition and diversity of soil microbial communities

Further soil subsamples were immediately frozen after sampling. DNA was extracted from soil samples using the DNeasy PowerSoil HTP 96 well DNA isolation kit (Qiagen, France) following the manufacturer's instructions. Quantification of the extracted DNA was performed using the Quant-IT dsDNA HS Assay Kit (Invitrogen, Carlsbad, CA, USA). The V3–V4 region of the 16S rRNA gene was amplified using the primers 341F (5′-CCTACGGGRSGCAGCAG-3′) and 805R (5′-GACTACCAGGGTATCTAAT-3′). The fungal ITS2 region was amplified using the primers ITS3F (5′-GCATCGATGAAGAACGCAGC-3′) and ITS4R (5′-TCCTCSSCTTATTGATATGC-3′). Amplicons were generated using a two-step PCR approach (Berry et al. 2011) and under PCR thermocycling conditions as described in (Romdhane et al. 2022). After checking the size of the PCR amplicons on a 2% agarose gel, the final PCR products were purified and their concentrations normalized using the SequalPrep Normalisation plate kit (Invitrogen, Carlsbad, CA, USA). Sequencing was performed on an Illumina MiSeq (2 × 250 bp) using the MiSeq Reagent Kit v2. Demultiplexing of samples and trimming of Illumina adapters and barcodes were performed with the Illumina MiSeq Reporter Software (version 2.5.1.3). Sequences were processed using an in-house Python pipeline (https://forgemia.inra.fr/vasa/illuminametabarcoding). Briefly, paired-end sequences were assembled using PEAR (version 0.9.8) (Zhang et al. 2014) with default settings. Further sequence

quality checks, including elimination of short sequences (< 400 bp for 16S and < 300 bp for ITS), were performed using the QIIME pipeline (version 1.9.1) (Caporaso et al. 2010). Reference-based and de novo chimera detection and OTU clustering were performed using VSEARCH (version 2.14.2) (Rognes et al. 2016) and the SILVA representative sequence set for 16S and UNITE's ITS2 reference dynamic dataset for ITS. Thresholds for OTU picking were set at 94% for 16S and 97% for ITS based on replicate sequencing of a bacterial mock community (Romdhane et al. 2022). Taxonomy was assigned using UCLUST (USEARCH version 11) (Edgar 2010) and the SILVA database (version 138.1/2020) (Quast et al. 2013) for 16S and BLAST (Altschul et al. 1990) and the UNITE reference database (version 8.3/2021) (Nilsson et al. 2019) for ITS. Sequences from the 16S rRNA gene that were classified as mitochondria or chloroplasts were excluded from the analysis.

After the initial sequence processing, 8 070 OTUs (59 946 ± 7 774 (average ± s.d.) reads per sample) and 5 820 OTUs (30 585 ± 5 343 reads per sample) were generated for 16S rRNA and ITS, respectively. Alpha diversity (i.e., OTU richness and Shannon index) was calculated after rarefaction to 41,000 reads per sample for 16S and 20,000 for ITS. Samples under rarefaction limits were excluded from the analyses.

Data processing and statistics

Gas concentration data from the experiments were processed using a custom R-script to calculate trace gas fluxes (Subramaniam et al. 2024). Statistical analysis was performed using a repeated-measures paired t-test with a significance level of 0.05 to assess the effects of elevated NO concentrations on soil-atmosphere trace gas fluxes and to compare cumulative fluxes between control and NO-flushed soils. IBM SPSS Statistics 27.0 was used to identify significant differences in trace gas fluxes between control [NO_0] and treated [NO_{200} or NO_{400}] mesocosms. In addition, simple t-tests were used to compare cumulative fluxes across the entire dataset and within each phase (P1–P6). All graphical representations of the data, including gas flux graphs, were generated using OriginPro 2020b (OriginLab Corporation, Northampton, MA, USA).

For metagenomic analysis, principal Coordinates Analysis (PCoA) and permutational multivariate analysis of variance (PERMANOVA) were calculated using Bray–Curtis dissimilarity matrices. Beta diversity PCoA plots were constructed using phyloseq (version 1.48.0) (McMurdie and Holmes 2013) using rarefied tables. PERMANOVAs were performed on the same rarefied matrices using the adonis2 function (999 permutations) in vegan (version 2.6–6.1) (Oksanen et al. 2024). Pairwise differences in bacterial and fungal composition were analyzed using the pairwise.adonis function (999 permutations, corrected $p < 0.05$ with FDR) of the pairwiseAdonis (version 0.4.1) package (Martinez Arbizu 2020). Taxonomic bar plots were calculated using microeco (version 1.9.0) (Liu et al. 2021). Differences in alpha diversity were assessed using non-parametric Kruskal–Wallis tests followed by Fisher's least significant difference with Benjamini–Hochberg correction ($p < 0.05$).

Results

Gas fluxes from the plant-free soil experiment

Soil NO emissions

Both NO emission dynamics and emission levels were remarkably similar for the two subsequent experiments, with only minor, quantitatively irrelevant effects of exogenous soil NO levels (Fig. 3). This was true for both the 200 and the 400 ppbv-NO concentrations. NO emissions generally increased linearly after increasing WFPS from 20 to 40% but had returned to background levels close to 0 after the first soil flush with exogenous NO. After fertigation, a clear NO peak was visible, with peak height shape, and tailing being unaffected by NO levels. Statistically significant differences between treatments at the end of the incubation were found only at minimal emission rates close to 0 and were thus quantitatively irrelevant.

Soil CO_2 emissions

Similar to the measured NO emission dynamics, also CO_2 emissions were not affected by exogenous NO levels, regardless of whether 200 or 400 ppbv-NO were established in the soil during the flushing periods. Again, the reproducibility of flux dynamics in the two

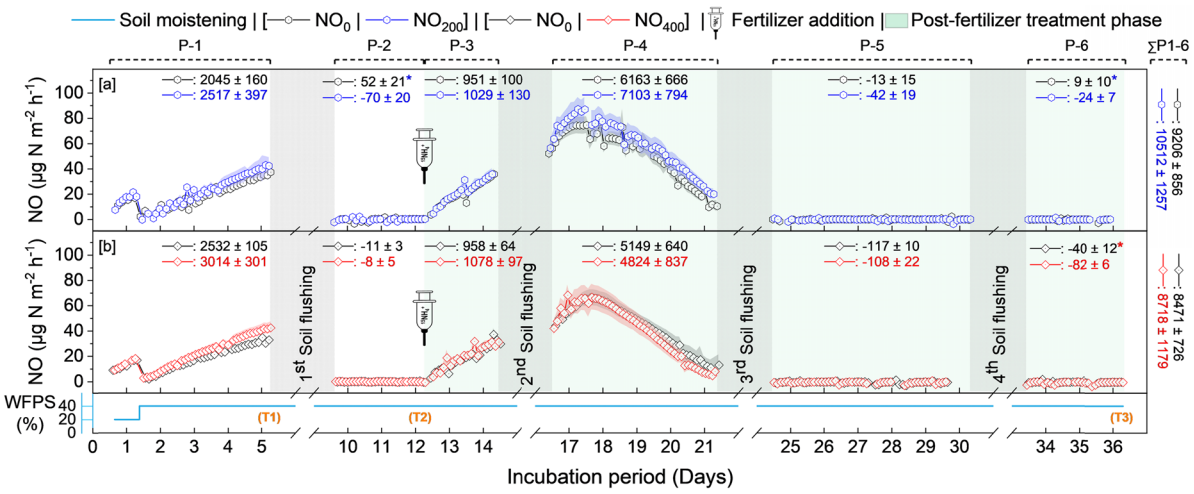

Fig. 3 The impact of different soil NO concentrations on soil-headspace exchange of NO in subsequent headspace flushing periods. Panel **a** compares NO_0 and NO_{200} treatments, while panel **b** contrasts NO_0 and NO_{400} treatments. The four "soil flushing" intervals are periods of setting soil NO concentrations, with no soil-headspace exchange measurements. Cumulative emissions for each measurement phase (P1-P6) are displayed in the graphs, with total cumulative emissions summarized at the end (ΣP1-P6). Soil sampling events are indicated as T1, T2, and T3. Data are presented as mean ± standard error (SE) based on six replicates (N = 6) with an asterisk (*) indicating statistical significance

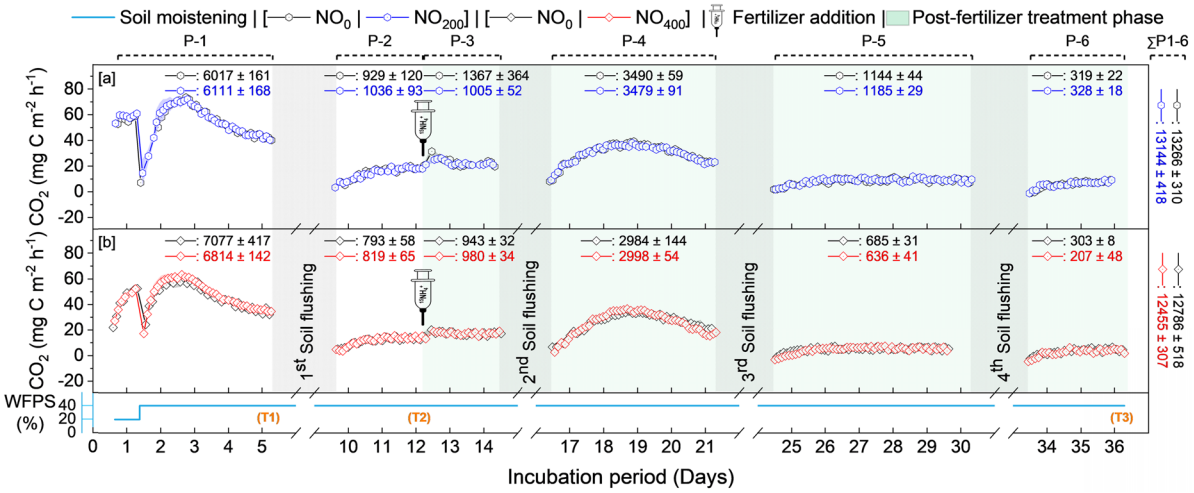

Fig. 4 The impact of varying soil NO concentrations on soil-headspace exchange of CO_2 in subsequent headspace flushing periods. Panel **a** compares NO_0 and NO_{200} treatments, while panel **b** contrasts NO_0 and NO_{400} treatments. The four "soil flushing" intervals are periods of setting soil NO concentrations, with no soil-headspace exchange measurements. Cumulative emissions for each measurement phase (P1-P6) are displayed in the graphs, with total cumulative emissions summarized at the end (ΣP1-P6). Soil sampling events are indicated as T1, T2, and T3. Data are presented as mean ± standard error (SE) based on six replicates (N = 6) with an asterisk (*) indicating statistical significance

subsequent incubations was remarkable, suggesting that similar soil microbial events occurred for the two exogenous NO levels despite the subsequent incubations. Interestingly, CO_2 emission was more affected by increasing WFPS rather than by the fertigation (Fig. 4).

Soil N_2O emissions

N_2O emissions increased sharply after WFPS had increased from 20 to 40% and decreased again to stabilize at a higher level (Fig. 5). In contrast, N_2O emissions increased slowly after fertigation to a broad peak that did not decline until about 2 weeks later. The sharp peak response to water addition was probably elevated in the control treatment compared to soils of the NO_{400} treatment, indicating minor initial treatment differences, but this remained unclear because the peak was not fully captured due to instrument failure. In contrast to NO and CO_2 emissions, we found that exogenous NO levels of 400 ppbv significantly reduced N_2O emissions during this peak period by more than 1/3, while this effect was not observed under exogenous NO levels of 200 ppbv (Fig. 5).

We also measured NO_2 (Fig. S1) and methane (CH_4) (Fig. S2) fluxes, but these remained consistently close to 0 and near the detection limit throughout the study and were also unaffected by NO concentrations. These results indicate that CH_4 and NO_2 were not important fluxes under the experimental conditions.

Soil-dissolved mineral nitrogen, organic nitrogen, and carbon

Initial N concentrations (T1 - before the first soil NO flushing) were 0.4 g NH_4^+-N m^{-2} and 1.2 g NO_3^--N m^{-2}. By day 13 (T2; after the first soil NO flush but before fertilization), the NH_4^+ levels had decreased to less than 0.1 g NH_4^+-N m^{-2} in both treatments.

The NO_3^- concentrations increased during the incubations mainly due to an increase after T2, i.e., after fertigation with NH_4^+ solution (Fig. 6). However, the NO_3^- concentrations as well as net nitrification rates throughout the incubation period were not influenced by the incubation period were not influenced by soil NO concentrations. DON concentrations showed similar temporal dynamics and were also not significantly affected by NO. (Fig. 6c) (Fig. 6d). The size of the MBN pools showed variable responses to NO concentrations. Microbial biomass

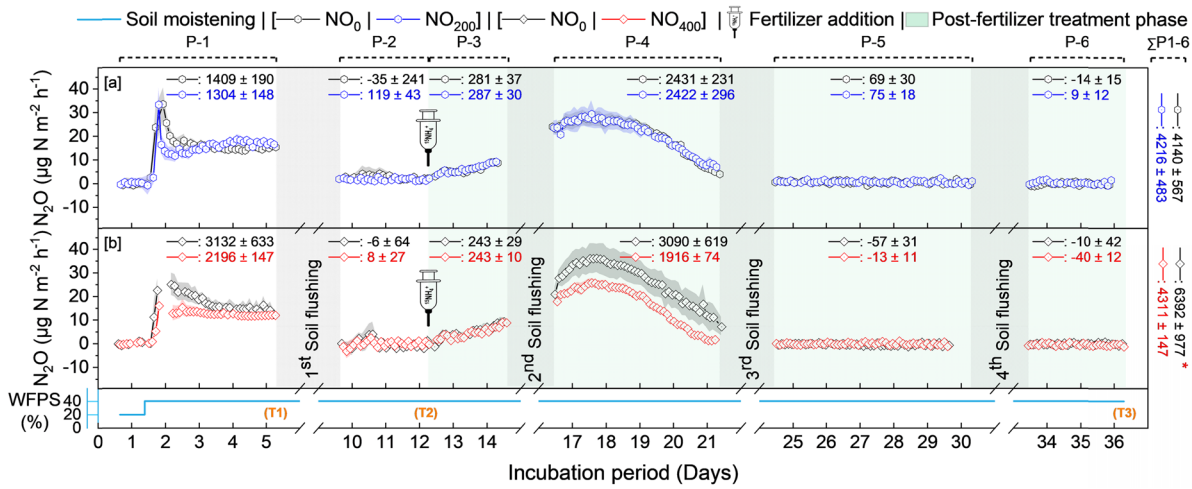

Fig. 5 The impact of adjusting varying soil NO concentrations on soil-headspace exchange of N_2O in subsequent headspace flushing periods. Panel **a** compares NO_0 and NO_{200} treatments, while panel **b** contrasts NO_0 and NO_{400} treatments. The four "soil flushing" intervals are periods of setting soil NO concentrations, with no soil-headspace exchange measurements. Cumulative emissions for each measurement phase (P1-P6) are displayed in the graphs, with total cumulative emissions summarized at the end (ΣP1-P6). Soil sampling events are indicated as T1, T2, and T3. Data are presented as mean ± standard error (SE) based on six replicates (N = 6) with an asterisk (*) indicating statistical significance

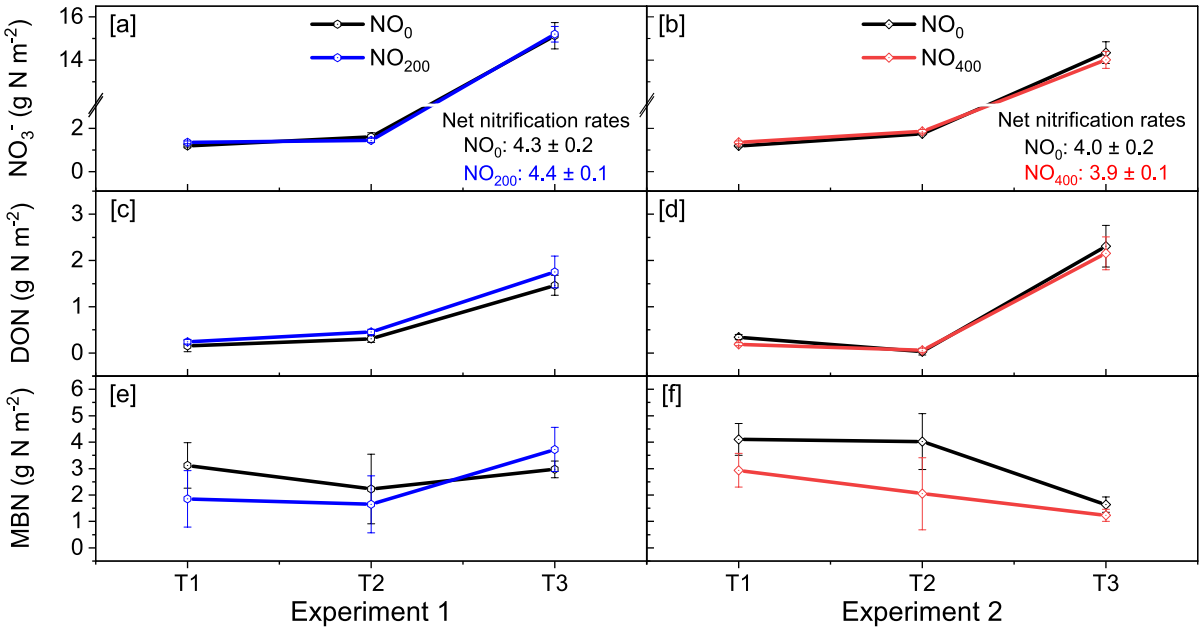

Fig. 6 Soil nitrate (NO_3^-) concentration and net nitrification rates (**a**, **b**), dissolved organic nitrogen (DON) concentrations (**c**, **d**), and microbial biomass nitrogen (MBN) concentration (**e, f**) for 200 ppbv-NO (left panels) and 400 ppbv-NO (right panels) compared to 0 ppbv-NO controls. Ammonium (NH_4^+) was partly not detectable due to low nitrogen concentrations and therefore is not shown. Fertigation was performed immediately following the T2 sampling. Data are presented as mean ± standard error (SE), based on six replicates (N = 6)

N (Fig. 6e) showed an almost significant reduction ($p = 0.06$) in the NO_{400} treatment (Fig. 6e), with values of 1.2 g MBN m^{-2} compared to 1.6 g MBN m^{-2} in the NO_0 treatment. Furthermore, MBN decreased in the course of the experiment at 400 ppbv exogenous NO. In contrast, in the NO_{200} treatment, we did not find such a decrease compared to the control, and the temporal trend in the experimental incubation showed an increase in MBN (Fig. 6e).

In summary, all the soil parameters showed no response to soil NO levels, except for the outlined contrasting responses of MBN at NO_{200} and NO_{400}.

^{15}N-fertilizer balance in the plant-free soil experiment

The ^{15}N fertilizer recovery in soil TN at the end of the experiment ranged from 79 and 84% and was not affected by manipulation of soil NO levels. This was in good accordance with the sum of ^{15}N excess recovery in extractable soil N pools such as mineral N, DON, and MBN (Table 1). This total ^{15}N fertilizer excess recovery was largely dominated by NO_3^- (ca. 65–70%), followed by MBN (ca. 10–20%) and DON (1–4%). In contrast, ^{15}N-recovery in NH_4^+ was undetectable due to low N concentrations, indicating that all applied $^{15}NH_4^+$ was largely nitrified, with a smaller fraction taken up by microorganisms. At 200 ppbv we found a more than doubled ^{15}N recovery in MBN in the topsoil compared to NO_0, which was still statistically significant when considering the whole soil depth (Table 1). Interestingly, the opposite effect was found at higher exogenous NO levels of 400 ppbv, i.e., a statistically significant reduction of ^{15}N excess recovery in MBN compared to the control in the 0–5 cm soil layer (Table 1).

Except for lower ^{15}N recovery in MBN at NO_{400} and higher ^{15}N recovery in MBN at NO_{200}, exogenous NO did not affect fertilizer ^{15}N recovery in the N pools analyzed.

Table 1 RGR^{15}N fertilizer recovery (% of applied ^{15}N excess)

The table presents the ^{15}N recovery % of both Experiment 1 and Experiment 2, including nitrate (NO_3^-), dissolved organic nitrogen (DON), microbial biomass nitrogen (MBN), and total nitrogen (TN) across two soil depth segments (0–5 cm and 5–10 cm). It also summarizes the total (Σ) recovery in NO_3^-, DON, and MBN, as well as cumulative recovery across depths, under varying NO treatments. Values are reported as mean ± standard error (SE) based on six replicates (N = 6), with statistically significant differences indicated by an asterisk (*) and in bold

Nitrogen Forms	Nitric oxide treatment	^{15}N recovery % (0–5 cm)	^{15}N recovery % (5–10 cm)	^{15}N recovery % Total Depth
NO_3^-	NO_0	54 ± 2	17 ± 3	70 ± 2
	NO_{200}	50 ± 2	18 ± 1	68 ± 2
	NO_0	54 ± 3	17 ± 2	71 ± 4
	NO_{400}	50 ± 2	19 ± 1	69 ± 2
DON	NO_0	3.0 ± 0.6	0.2 ± 0.0	2.7 ± 0.7
	NO_{200}	3.4 ± 1.0	0.3 ± 0.2	3.7 ± 0.9
	NO_0	3.2 ± 0.7	1.2 ± 0.5	4.4 ± 0.8
	NO_{400}	2.3 ± 0.5	0.9 ± 0.1	3.3 ± 0.6
MBN	NO_0	**8.8 ± 1.4 ***	5.6 ± 0.6	**14.3 ± 1.7 ***
	NO_{200}	**18.4 ± 3.6**	4.3 ± 1.1	**22.6 ± 3.5**
	NO_0	**7.5 ± 0.7 ***	3.5 ± 1.0	11.1 ± 1.5
	NO_{400}	**5.4 ± 0.8**	3.6 ± 0.2	9.0 ± 0.8
TN	NO_0	62 ± 3	22 ± 1	84 ± 2
	NO_{200}	65 ± 2	19 ± 1	84 ± 1
	NO_0	62 ± 2	20 ± 1	82 ± 2
	NO_{400}	59 ± 2	20 ± 0	79 ± 2
Σ (NO_3^-, DON, MBN)	NO_0	65.8 ± 2.5	22.8 ± 3.1	87 ± 2.7
	NO_{200}	71.8 ± 4.2	22.6 ± 1.5	94.3 ± 4.1
	NO_0	64.7 ± 3.2	21.7 ± 2.3	86.5 ± 4.3
	NO_{400}	57.7 ± 2.2	23.5 ± 1.0	81.3 ± 2.2

Effects of soil flushing with NO on soil microbial community

Soil flushing with 200 ppbv-NO and 400 ppbv-NO did not alter the relative abundance of the major bacterial and fungal phyla, which varied with experiment, incubation time, or soil depth (Fig. 7). The bacterial communities were dominated by *Firmicutes* (36–45%), followed by *Actinobacteria* (12–14%) and *Gammaproteobacteria* (10–12%) (Fig. 7a), whereas the fungal communities were dominated by *Ascomycota* (47–58%), followed by *Basidiomycota* (18–25%) (Fig. 7b). Importantly, no significant effects of NO treatments were detected on overall microbial diversity or community composition, indicating that neither 200 ppbv nor 400 ppbv of exogenous NO reshaped the structure of the bacterial or fungal communities. Also the OTU richness of the bacterial or fungal communities did not change with exogenous soil NO concentrations at either 200 ppbv-NO or 400 ppbv-NO compared to 0 ppbv-NO, but varied depending on the experiment and incubation time (Fig. 8). The number of bacterial OTUs increased with time in the experiment with 400 ppbv-NO, but not in the experiment with 200 ppbv-NO (Fig. 8a). OTU richness of the fungal communities did not increase with time except in control samples at 5 cm depth and T3 in the 0–200 ppbv-NO experiment (Fig. 8b). Similarly, no significant effects of increasing NO concentration were detected on the beta diversity of the bacterial and fungal communities as visualized by principal coordinate analysis (PCoA) and tested by a permutational multivariate analysis of variance (PERMANOVA) (Fig. 9, Table S1). At the surface or to a depth of 5 cm, the bacterial beta diversity only varied significantly with time in both the 200 ppbv-NO and 400 ppbv-NO experiments, while it also varied with soil depth at T3 (Fig. 9a). Fungal beta diversity also varied significantly with time and soil depth, but only in the 200 ppbv-NO experiment (Fig. 9b).

Discussion

Effects of NO on soil C and N cycling

The main effect of different NO levels was an increase in fertilizer ^{15}N uptake into MBN at 200

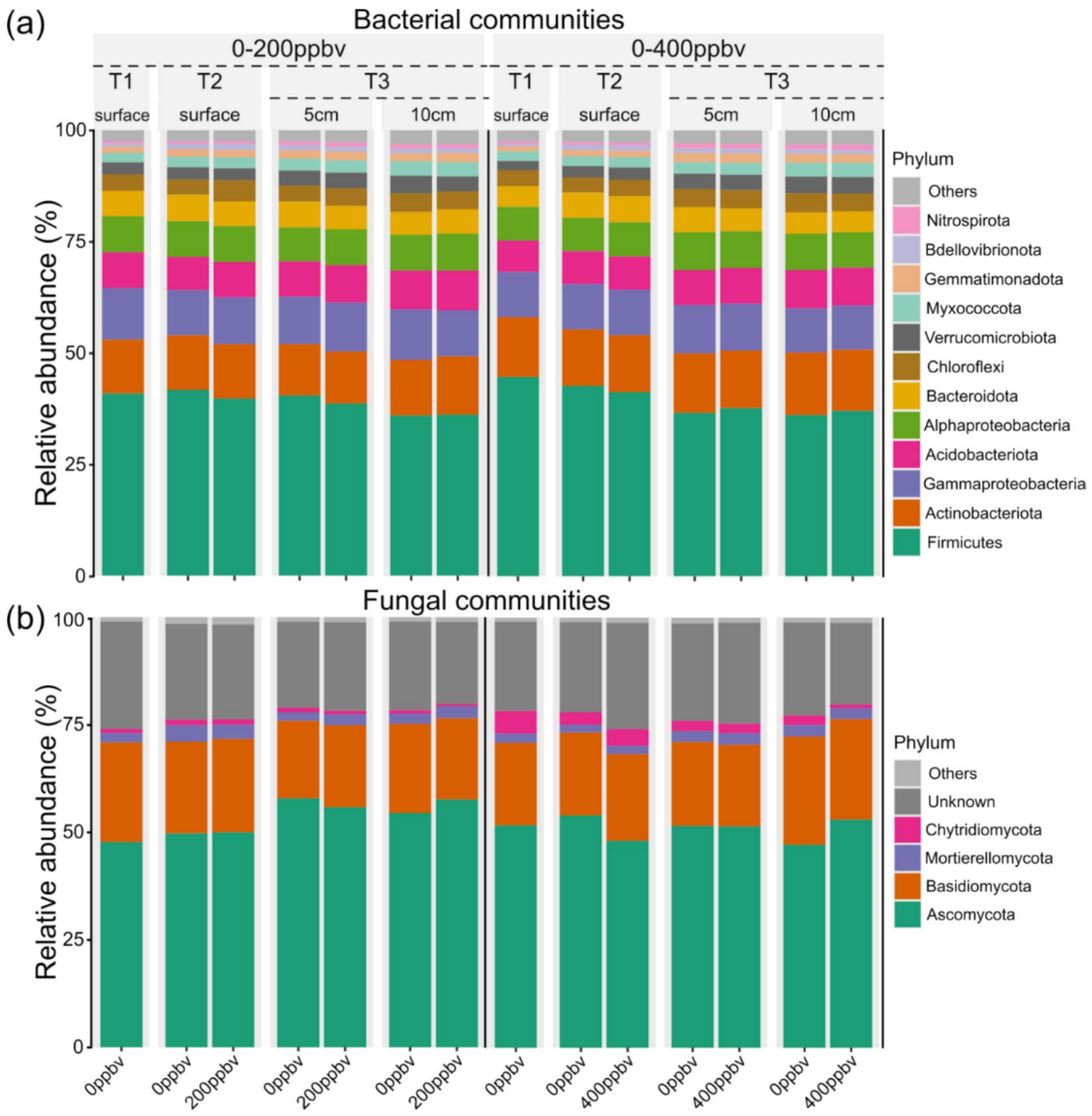

Fig. 7 Relative abundance (in percentage) of the (**a**) twelve most abundant bacterial phyla (class for Proteobacteria) and the (**b**) five most abundant fungal phyla as measured in the soil of the mesocosm experiments after flushing with 0–200 ppbv-NO and 0–400 ppbv-NO. The category others cluster taxa from less abundant phyla

ppbv-NO, whereas the opposite effect was observed at 400 ppbv-NO: a decrease in MBN and microbial ^{15}N uptake as determined by chloroform-fumigation extraction, accompanied by lower N_2O emissions. These contrasting responses of microbial N turnover processes at the two NO levels suggest different mechanisms triggered by NO effects on soil N turnover processes, particularly inorganic N assimilation, with a threshold value for the two mechanisms existing between 200 and 400 ppbv exogenous NO. Due to its multifaceted role as a signaling agent, at 200 ppbv exogenous NO could have stimulated microbial N metabolism including enhanced heterotrophic inorganic N assimilation (Medinets et al.

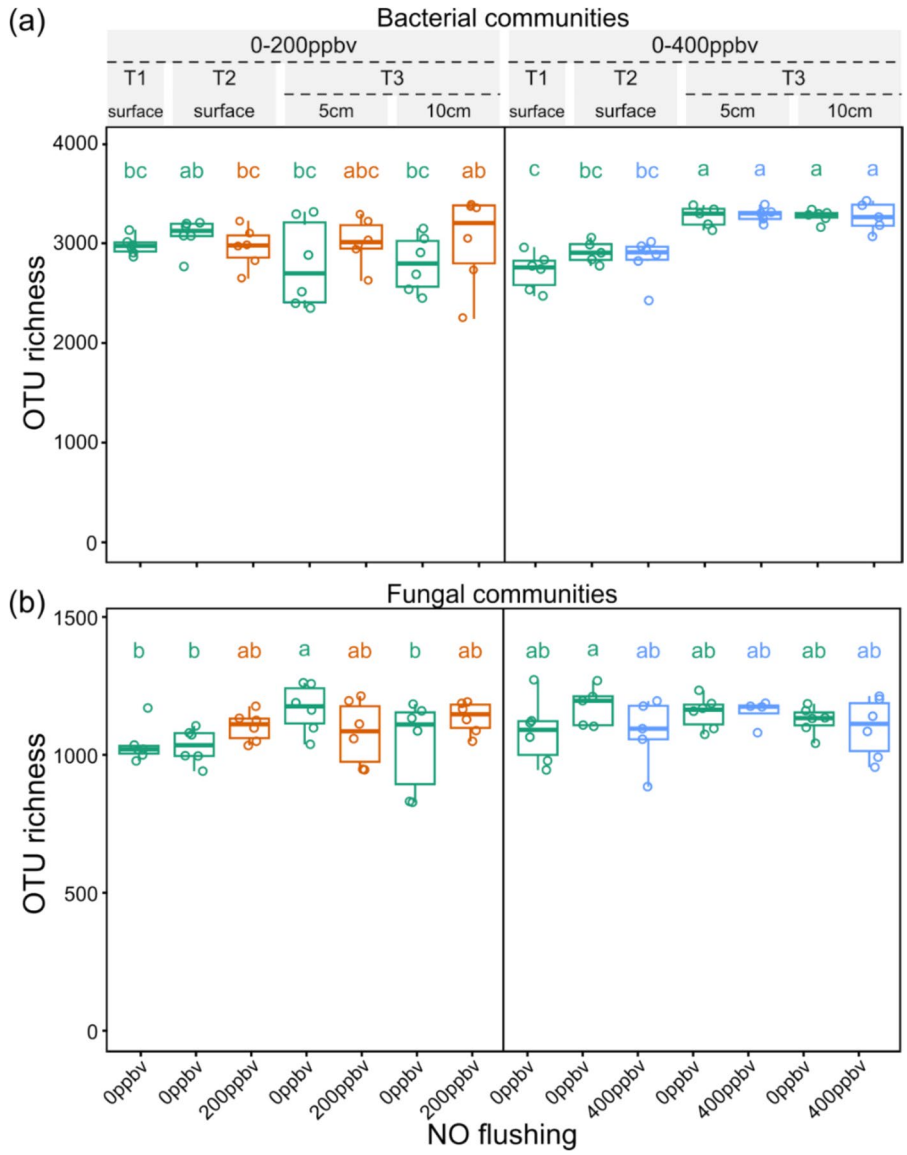

Fig. 8 Boxplot showing the (**a**) bacterial and (**b**) fungal OTU richness in two mesocosm experiments conducted with soil after flushing with 0 vs. 200 ppbv NO and 0 vs. 400 ppbv NO. Distinct letters above the boxes indicate significant differences based on non-parametric Kruskal–Wallis tests, followed by Fisher's least significant difference with Benjamini–Hochberg correction ($p < 0.05$)

2015). This would be possible due to the diffusive properties of NO, allowing exogenous NO to enhance the functions of cell-endogenous NO produced by the NOS enzyme, whereas in the NO_0 treatment, the physiological cell functioning would be based solely on endogenous NO (Medinets et al. 2015). This indicates a signaling vs. toxicity threshold between 200 and 400 ppbv NO so that its role changed from enhancing microbial N assimilation (Gupta et al. 2022) at 200 ppbv to the induction of cellular stress or enzymatic disruption at 400 ppbv, thereby microbial N assimilation (Conrad 1995). Thus, the contrasting effects at 400 ppbv exogenous NO – i.e., reduced MBN and ^{15}N uptake and N_2O emissions, are likely to result from an inhibitory effect of high NO concentrations on microbial activity, with however no detoxification being visible in the form of increased N_2O emissions. It should be noted that NO detoxification via reduction to N_2O does not necessarily result in measurable additional net N_2O emissions in case N_2O is predominantly reduced to N_2. However, given the high NO_3^- concentrations and low WFPS values under the prevailing experimental conditions, which should largely have prevented N_2O reductase activity in the course of heterotrophic denitrification (Butterbach-Bahl et al. 2013), this would have been rather

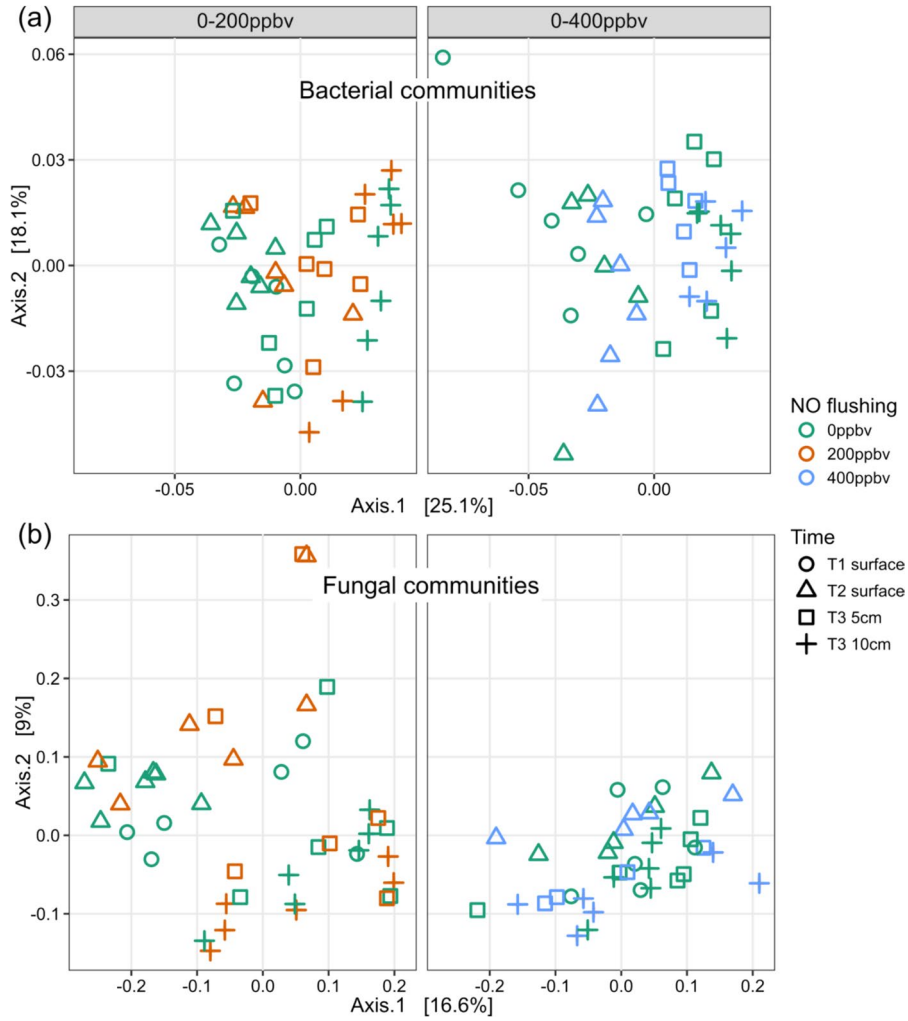

Fig. 9 PCoA analyses of Bray–Curtis dissimilarities in (**a**) bacterial and (**b**) fungal communities in two mesocosm experiments conducted with soil after flushing with 0 vs. 200 ppbv-NO and 0 vs. 400 ppbv-NO

unlikely in our study. Under conditions of high N availability, low organic C content, also nitrifier-denitrification by AOB can facilitate the stepwise reduction of NO_2^- to NO, N_2O, and finally N_2 (Remde and Conrad 1990; Wrage et al. 2001), which however also appears unlikely to have masked NO detoxification in our incubations. Instead, reduced N_2O emissions as observed here at 400 ppbv NO concentrations could be explained by inhibitory effects of NO on N_2O formation from Nor enzyme activity, e.g., via formation of nitrosyl complexes (Hayashi et al. 2007; Hendriks et al. 1998; Vollack and Zumft 2001). Besides, mechanisms such as NO-binding proteins and reversible S-nitrosation (Gusarov and Nudler 2012) may have mitigated NO toxicity, thereby contributing to reduced N_2O formation. Furthermore, reactive soil minerals, including manganese oxides, could have detoxified NO by oxidizing it to NO_3^-, effectively bypassing denitrification and reducing N_2O production (Zhang et al. 2018), but such effects should probably have been visible also at 200 ppbv-NO. All of this remains somewhat speculative unless ^{15}N labeled NO is used and traced into N_2O in follow-up studies.

Although we exposed the soils in our experiments to NO concentrations typical for N-saturated soils for 12 days and measured a wide range of biogeochemical and molecular parameters, from detailed ^{15}N fertilizer tracing to C and N trace gas exchange and microbial community analysis, we found no further effects of NO. This indicates that, at least for the soil analyzed in this study and its specific C and N cycling patterns, there was little overall effect of exogenous NO additions on C and N biogeochemistry, with NO acting neither as a toxic nor as a signaling compound.

Our measurements indicate that autotrophic nitrification was the dominant process in our soils. The high rates of net nitrification and ^{15}N conversion to NO_3^-, remaining unaffected by exogenous NO, suggest that cell function in nitrifiers was facilitated by sufficient endogenous NO production (Medinets et al. 2015). This N cycling pattern is characteristic of soils with high oxygen and low C availability, which favors autotrophic nitrification over heterotrophic microbial activities, such as denitrification and inorganic N assimilation (Butterbach-Bahl and Dannenmann 2011 and 2012). This was also clearly demonstrated by the generally low ^{15}N uptake into microbial biomass and low soil respiration rates. Thus, the heterotrophic activity of free-living microorganisms, which is also important for competition with plants for inorganic N, was already impaired by limited C availability before the addition of exogenous NO. Therefore, further studies with more C-rich soils are needed to analyze the effects of NO on heterotrophic microbial activity and processes.

Limitations of the present study and recommendations for further studies

This study used an advanced soil-incubation system specifically designed for precise manipulation of soil NO concentrations, allowing for highly accurate measurements of greenhouse gas and reactive gas fluxes. The system's high-resolution capabilities and low detection limits facilitated the detection of subtle changes in emissions (Subramaniam et al. 2024). In addition, a meticulously conducted, well-contained ^{15}N fertilizer balance was used to accurately N transformations with precision. However, despite the use of these state-of-the-art methods, NO treatment effects were mainly limited to quantitatively small changes in N_2O emissions. On the one hand, this could indicate a limited effect of NO in soil systems compared to pure cultures, at least under the given experimental conditions. Even so, it could be due to methodological limitations that should be overcome in future studies.

First, the inherent technical setup of our system did not allow automated gas flux measurements while maintaining exogenous NO availability in the soil. Therefore, it would be desirable to have a system that allows for simultaneous soil and headspace flushing, combining exogenous NO manipulation with simultaneous C and N trace gas flux measurements. As longer-term microbial adaptations could not be captured in this short-term incubation study, we also recommend extending the NO soil flushing periods beyond the 12 days of this study.

Second, the range of exogenous NO concentrations was likely insufficient, also in light of the limited research available on in situ soil NO concentrations. (Medinets et al. 2019) reported peak soil air NO concentrations ranging from 492 to 800 ppbv in different soil layers under summer conditions, especially after rainfall in the Höglwald forest soil in southern Germany. Similarly, (Gut et al. 2002) observed NO concentrations ranging from 20 to 460 ppbv in Amazonian rainforest soils. In agricultural systems, (Gut et al. 1999) measured soil NO concentrations at a 2 cm depth in a wheat field fertilized with either 19 kg cattle slurry-N ha^{-1}, 40 kg N ha^{-1} from NH_4NO_3 fertilizer, or remaining unfertilized. They observed maximum NO concentrations of 85 ppbv following slurry application, 410 ppbv after NH_4NO_3 fertilization, and 63 ppbv in the unfertilized plot. This generally justifies the NO concentrations we applied, but we encourage the use of wider ranges of exogenous NO additions in future studies, including higher NO levels, when manipulating NO in experimental incubations. This is also because soil NO measurements are unlikely to capture the presumably very high NO concentrations in small-scale nitrification hot spots. Also, studies on biofilm formation (e.g., *Pseudomonas aeruginosa*), and dispersal suggest that this may depend on higher NO concentrations than used in this study (Arora et al. 2015).

Third, our pioneering study focused on only one specific soil. Given that this soil has an N cycle dominated by autotrophic nitrification and rather reduced heterotrophic microbial activity due to lack of available C and low water content, further research should focus on using more biologically active C-rich soils, such as those from grasslands, forests, or agricultural soils after residue incorporation. We also suggest assessing the role of NO at various soil WFPS.

Furthermore, the use of ^{15}N-labeled NO is recommended for future studies to gain more detailed insights into the fate of NO in plant-soil-microbe systems (Stark and Firestone 1995), especially its role as an electron acceptor during denitrification. Given the role of NO in plant metabolism, the role of plants

as NO source, and the potentially important role in plant-soil-microbe interactions (Medinets et al. 2015), the absence of plants in this study limits ecological extrapolation. Therefore, the inclusion of plants in the experimental design may on the one hand complicate the experimental setup, but is of paramount importance towards a quantitative understanding of the role of NO in plant-soil-systems.

Conclusion

This study revealed for agricultural soil that – compared to exogenous NO – 200 ppbv of exogenous NO stimulated fertilizer N uptake into microbial biomass, while the opposite effect was observed at 400 ppbv exogenous NO. This suggests an important, strongly concentration-dependent role of exogenous NO in nitrogen retention in agricultural soils, which however needs to be further investigated in future studies.

Acknowledgements Natalia Hordovska, Kilian Gal, and Marie Christine Breuil helped with sampling and laboratory work. This study was undertaken as part of the Franco-German Project NO-PIMS "What is the role of exogenous NO for plants, microbes, and their interactions in soil?". The project received financial support from the Deutsche Forschungsgemeinschaft (DFG) of Germany (BU 1173/25-1) and the Agence Nationale de la Recherche (ANR-20-CE92-0004) of France. Additional funding was provided to KBB by the Pioneer Center for Research in Sustainable Agricultural Futures (Land-CRAFT), under DNRF grant number P2.

Author contributions M.D., K.B.B., L.P., N.B., and L.S., designed the study, EP-V., A.B., performed microbial analyses and statistical analyses; U.O., performed EA-IRMS analyses; F.E. developed the mesocosm system and conducted trace gas flux measurements; L.S., executed the experiment, performed laboratory analyses and statistical analyses with the support of all authors, and drafted the manuscript. All authors discussed the results and contributed to the final document. Funding acquisition by K.B.B., M.D., L.P., and N.B.; L.S., and EP-V contributed equally to this work.

Funding Open Access funding enabled and organized by Projekt DEAL. This work was funded by Deutsche Forschungsgemeinschaft, BU 1173/25-1, Klaus Butterbach-Bahl, Agence Nationale de la Recherche, ANR-20-CE92-0004, Laurent Philippot

Data availability Raw sequence data of 16S rRNA and fungal ITS have been deposited in the Sequence Read Archive NCBI under BioProject accession numbers PRJNA1171373 and PRJNA1171410, respectively. The datasets generated and/or analyzed during the current study are available from the corresponding author upon reasonable request.

Declarations

Conflict of interests Declaration of absence of any competing interests or conflicts of interest among the authors.

References

Altschul SF, Gish W, Miller W, Myers EW, Lipman DJ (1990) Basic local alignment search tool. J Mol Biol 215:403–410. https://doi.org/10.1016/S0022-2836(05)80360-2

Amahisa M, Tsukagoshi M, Kadooka C, Masuo S, Takeshita N, Doi Y, Takagi H, Takaya N (2024) The metabolic regulation of amino acid synthesis counteracts reactive nitrogen stress via Aspergillus nidulans cross-pathway control. J Fungi 10:1. https://doi.org/10.3390/jof10010001

Arora DP, Hossain S, Xu Y, Boon EM (2015) Nitric oxide regulation of bacterial biofilms. Biochemistry 54:3717–3728. https://doi.org/10.1021/bi501476n

Bergaust L, Mao Y, Bakken LR, Frostegård Å (2010) Denitrification response patterns during the transition to anoxic respiration and posttranscriptional effects of suboptimal pH on nitrogen oxide reductase in *Paracoccus denitrificans*. Appl Environ Microbiol 76:6387–6396. https://doi.org/10.1128/AEM.00608-10

Berry D, Ben Mahfoudh K, Wagner M, Loy A (2011) Barcoded primers used in multiplex amplicon pyrosequencing bias amplification. Appl Environ Microbiol 77:7846–7849. https://doi.org/10.1128/AEM.05220-11

Borrero-de Acuña JM, Rohde M, Wissing J, Jänsch L, Schobert M, Molinari G, Timmis KN, Jahn M, Jahn D (2016) Protein network of the *Pseudomonas aeruginosa* denitrification apparatus. J Bacteriol 198:1401–1413. https://doi.org/10.1128/JB.00055-16

Borrero-de Acuña JM, Timmis KN, Jahn M, Jahn D (2017) Protein complex formation during denitrification by *Pseudomonas aeruginosa*. Microb Biotechnol 10:1523–1534. https://doi.org/10.1111/1751-7915.12851

Butterbach-Bahl K (2011) Nitrogen processes in terrestrial ecosystems. Eur Nitrogen Assess 6:1–27. https://doi.org/10.1016/j.cosust.2011.08.004

Butterbach-Bahl K, Dannenmann M (2011) Denitrification and associated soil N_2O emissions due to agricultural activities in a changing climate. Curr Opin Environ Sustain 3:389–395. https://doi.org/10.1016/j.cosust.2011.08.004

Butterbach-Bahl K, Dannenmann M (2012) Soil carbon and nitrogen interactions and biosphere-atmosphere exchange of nitrous oxide and methane. In: Lal R, Lorenz K, Hüttl RF, Schneider BU, von Braun J (eds) Recarbonization of the biosphere. Springer, Dordrecht, pp 429–443. https://doi.org/10.1007/978-94-007-4159-1_19

Butterbach-Bahl K, Baggs EM, Dannenmann M, Kiese R, Zechmeister-Boltenstern S (2013) Nitrous oxide emissions from soils: how well do we understand the processes and their controls? Philos Trans R Soc Lond B Biol Sci 368:20130122. https://doi.org/10.1098/rstb.2013.0122

Caporaso JG, Kuczynski J, Stombaugh J, Bittinger K, Bushman FD, Costello EK, Fierer N, Pena AG, Goodrich JK, Gordon JI, Huttley GA, Kelley ST, Knights D, Koenig JE, Ley RE, Lozupone CA, McDonald D, Muegge BD, Pirrung M, Reeder J, Sevinsky JR, Turnbaugh PJ, Walters WA, Widmann J, Yatsunenko T, Zaneveld J, Knight R (2010) QIIME allows analysis of high-throughput community sequencing data. Nat Methods 7:335–336. https://doi.org/10.1038/nmeth.f.303

Chiranand W, McLeod I, Zhou H, Lynn JJ, Vega LA, Myers H, Yates JR, Lorenz MC, Gustin MC (2008) CTA4 transcription factor mediates induction of nitrosative stress response in Candida albicans. Eukaryot Cell 7:268–278. https://doi.org/10.1128/EC.00240-07

Conrad R (1995) Soil microbial processes and the cycling of atmospheric trace gases. Philos Trans R Soc Lond A 351:219–230. https://doi.org/10.1098/rsta.1995.0030

Conrad R (1996) Metabolism of nitric oxide in soil and soil microorganisms and regulation of flux into the atmosphere. Microbiol Atmos Trace Gases 139:167–203. https://doi.org/10.1007/978-3-642-61096-7_11

Dannenmann M, Simon J, Gasche R, Holst J, Naumann PS, Kögel-Knabner I, Knicker H, Mayer H, Schloter M, Pena R, Polle A, Rennenberg H, Papen H (2009) Tree girdling provides insight on the role of labile carbon in nitrogen partitioning between soil microorganisms and adult European beech. Soil Biol Biochem 41:1622–1631. https://doi.org/10.1016/j.soilbio.2009.04.024

Dannenmann M, Bimüller C, Gschwendtner S, Leberecht M, Tejedor J, Bilela S, Gasche R, Hanewinkel M, Baltensweiler A, Kögel-Knabner I, Polle A, Schloter M, Simon J, Rennenberg H (2016) Climate change impairs nitrogen cycling in European beech forests. PLoS ONE 11:1–24. https://doi.org/10.1371/journal.pone.0158823

Dannenmann M, Díaz E, Barbara P, Kristiina K, Tejedor J, Ambus P, Parra A, Sánchez L, Resco V, Ramírez DA, Guimaraes LP, Willibald G, Gasche R, Zechmeister S, David B, Castaldi S, Vallejo A, Rubio A, Moreno JM, Bahl KB (2018) Postfire nitrogen balance of Mediterranean shrublands: direct combustion losses versus gaseous and leaching losses from the postfire soil mineral nitrogen flush. Glob Change Biol 24:4505–4520. https://doi.org/10.1111/gcb.14388

De Boer APN, Van Der Oost J, Reijnders WNM, Westerhoff HV, Stouthamer AH, Van Spanning RJM (1996) Mutational analysis of the nor gene cluster which encodes nitric-oxide reductase from *Paracoccus denitrificans*. Eur J Biochem 242:592–600. https://doi.org/10.1111/j.1432-1033.1996.0592r.x

De La Fuente-Núñez C, Reffuveille F, Fairfull-Smith KE, Hancock REW (2013) Effect of nitroxides on swarming motility and biofilm formation, multicellular behaviors in *Pseudomonas aeruginosa*. Antimicrob Agents Chemother 57:4877–4881. https://doi.org/10.1128/AAC.01381-13

Edgar RC (2010) Search and clustering orders of magnitude faster than BLAST. Bioinformatics 26:2460–2461. https://doi.org/10.1093/bioinformatics/btq461

Fowler D, Pilegaard K, Sutton MA, Ambus P, Raivonen M, Duyzer J, Simpson D, Fagerli H, Fuzzi S, Schjoerring JK, Granier C, Neftel A, Isaksen ISA, Laj P, Maione M, Monks PS, Burkhardt J, Daemmgen U, Neirynck J, Erisman JW (2009) Atmospheric composition change: ecosystems-atmosphere interactions. Atmos Environ 43:5193–5267. https://doi.org/10.1016/j.atmosenv.2009.07.068

Ghaffari A, Miller CC, McMullin B, Ghahary A (2006) Potential application of gaseous nitric oxide as a topical antimicrobial agent. Nitric Oxide 14:21–29. https://doi.org/10.1016/j.niox.2005.08.003

Gopalasingam CC, Johnson RM, Chiduza GN, Tosha T, Yamamoto M, Shiro Y, Antonyuk SV, Muench SP, Hasnain SS (2019) Dimeric structures of quinol-dependent nitric oxide reductases (qNORs) revealed by cryo–electron microscopy. Sci Adv 5:eaax1803. https://doi.org/10.1126/sciadv.aax1803

Groffman PM, Altabet MA, Böhlke JK, Butterbach-Bahl K, David MB, Firestone MK, Giblin AE, Kana TM, Nielsen LP, Voytek MA (2006) Methods for measuring denitrification: diverse approaches to a difficult problem. Ecol Appl 16:2091–2122. https://doi.org/10.1890/1051-0761(2006)016[2091:MFMDDA]2.0.CO;2

Gupta A, Singh UB, Sahu PK, Paul S, Kumar A, Malviya D, Singh S, Kuppusamy P, Singh P, Paul D, Rai JP, Singh HV, Manna MC, Crusberg TC, Kumar A, Saxena AK (2022) Linking soil microbial diversity to modern agriculture practices: a review. Int J Environ Res Public Health 19:3141. https://doi.org/10.3390/ijerph19053141

Gusarov I, Nudler E (2012) S-nitrosylation signaling in *Escherichia coli*. Sci Signal 5:3–5. https://doi.org/10.1126/scisignal.2003181

Gut A, Neftel A, Staffelbach T, Riedo M, Lehmann BE (1999) Nitric oxide flux from soil during the growing season of wheat by continuous measurements of the NO soil-atmosphere concentration gradient: a process study. Plant Soil 216:165–180. https://doi.org/10.1023/a:1004752104808

Gut A, van Dijk SM, Scheibe M, Rummel U, Welling M, Ammann C, Meixner FX, Kirkman GA, Andreae MO, Lehmann BE (2002) NO emission from an Amazonian rain forest soil: continuous measurements of NO flux and soil concentration. J Geophys Res Atmos 107:LBA24-1-LBA24-10. https://doi.org/10.1029/2001JD000521

Hayashi T, Lin IJ, Chen Y, Fee JA, Moënne-Loccoz P (2007) Fourier transform infrared characterization of a CuB-nitrosyl complex in cytochrome ba3 from *Thermus thermophilus*: relevance to NO reductase activity in heme-copper terminal oxidases. J Am Chem Soc 129:14952–14958. https://doi.org/10.1021/ja074600a

Heil J, Vereecken H, Brüggemann N (2016) A review of chemical reactions of nitrification intermediates and their role in nitrogen cycling and nitrogen trace gas formation in soil. Eur J Soil Sci 67:23–39. https://doi.org/10.1111/ejss.12306

Hendriks J, Warne A, Gohlke U, Haltia T, Ludovici C, Lübben M, Saraste M (1998) The active site of the bacterial nitric oxide reductase is a dinuclear iron center. Biochemistry 37:13102–13109. https://doi.org/10.1021/bi980943x

Hino T, Matsumoto Y, Nagano S, Sugimoto H, Fukumori Y, Murata T, Iwata S, Shiro Y (2010) Structural basis of biological N_2O generation by bacterial nitric oxide reductase. Science 330:1666–1670. https://doi.org/10.1126/science.1195591

IUSS Working Group WRB (2022) World reference base for soil resources. International soil classification system for naming soils and creating legends for soil maps. International Union of Soil Sciences (IUSS), 4th edn. Vienna, Austria

Jackson MA, Tiedje JM, Averill BA (1991) Evidence for an NO-rebound mechanism for production of N_2O from nitrite by the copper-containing nitrite reductase from Achromobacter cycloclastes. FEBS Lett 291:41–44. https://doi.org/10.1016/0014-5793(91)81099-T

Ji Y, Neverova I, Van Eyk JE, Bennett BM (2006) Nitration of tyrosine 92 mediates the activation of rat microsomal glutathione Stransferase by peroxynitrite. J Biol Chem 281:1986–1991. https://doi.org/10.1074/jbc.M509480200

Jones LC, Peters B, Lezama Pacheco JS, Casciotti KL, Fendorf S (2015) Stable isotopes and iron oxide mineral products as markers of chemodenitrification. Environ Sci Technol 49:3444–3452. https://doi.org/10.1021/es504862x

Korner H, Zumft WG (1989) Expression of denitrification enzymes in response to the dissolved oxygen levels and respiratory substrate in continuous culture of *Pseudomonas stutzeri*. Appl Environ Microbiol 55:1670–1676. https://doi.org/10.1128/aem.55.7.1670-1676.1989

Lionetti D, De Ruiter G, Agapie T (2016) A trans-hyponitrite intermediate in the reductive coupling and deoxygenation of nitric oxide by a tricopper-Lewis acid complex. J Am Chem Soc 138:5008–5011. https://doi.org/10.1021/jacs.6b01083

Liu C, Cui Y, Li X, Yao M (2021) Microeco: an R package for data mining in microbial community ecology. FEMS Microbiol Ecol 97:fiaa255. https://doi.org/10.1093/femsec/fiaa255

Ma M, Wendehenne D, Philippot L, Hänsch R, Flemetakis E, Hu B, Rennenberg H (2020) Physiological significance of pedospheric nitric oxide for root growth, development, and organismic interactions. Plant Cell Environ 43:2336–2354. https://doi.org/10.1111/pce.13850

Martens-Habbena W, Qin W, Horak REA, Urakawa H, Schauer AJ, Moffett JW, Armbrust EV, Ingalls AE, Devol AH, Stahl DA (2015) The production of nitric oxide by marine ammonia-oxidizing archaea and inhibition of archaeal ammonia oxidation by a nitric oxide scavenger. Environ Microbiol 17:2261–2274. https://doi.org/10.1111/1462-2920.12677

Martinez Arbizu P (2020) pairwiseAdonis: Pairwise multilevel comparison using adonis. R Package Version 0.4 1.

Mayburd AL, Kassner RJ (2002) Mechanism and biological role of nitric oxide binding to cytochrome c′. Biochemistry 41:11582–11591. https://doi.org/10.1021/bi020058l

McMurdie PJ, Holmes S (2013) Phyloseq: an R package for reproducible interactive analysis and graphics of microbiome census data. PLoS ONE 8:e61217. https://doi.org/10.1371/journal.pone.0061217

Medinets S, Skiba U, Rennenberg H, Butterbach-Bahl K (2015) A review of soil NO transformation: associated processes and possible physiological significance on organisms. Soil Biol Biochem 80:92–117. https://doi.org/10.1016/j.soilbio.2014.09.025

Medinets S, Gasche R, Kiese R, Rennenberg H, Butterbach-Bahl K (2019) Seasonal dynamics and profiles of soil NO concentrations in a temperate forest. Plant Soil 445:335–348. https://doi.org/10.1007/s11104-019-04305-5

Miller CC, Miller MK, Ghaffari A, Kunimoto B (2004) Treatment of chronic nonhealing leg ulceration with gaseous nitric oxide: a case study. J Cutan Med Surg 8:233–238. https://doi.org/10.1007/s10227-004-0106-8

Miller C, McMullin B, Ghaffari A, Stenzler A, Pick N, Roscoe D, Ghahary A, Road J, Av-Gay Y (2009) Gaseous nitric oxide bactericidal activity retained during intermittent high-dose short-duration exposure. Nitric Oxide 20:16–23. https://doi.org/10.1016/j.niox.2008.08.002

Nilsson RH, Larsson K-H, Taylor AFS, Bengtsson-Palme J, Jeppesen TS, Schigel D, Kennedy P, Picard K, Glöckner FO, Tedersoo L, Saar I, Kõljalg U, Abarenkov K (2019) The UNITE database for molecular identification of fungi: handling dark taxa and parallel taxonomic classifications. Nucleic Acids Res 47(D1):D259–D264. https://doi.org/10.1093/nar/gky1022

Oksanen J, Simpson GL, Blanchet FG, Kindt R, Legendre P, Minchin PR, O'Hara RB, Solymos P, Stevens MH, Szoecs E, Wagner H, Barbour M, Bedward M, Bolker B, Borcard D, Carvalho G, Chirico M, De Caceres M, Durand S, Evangelista HBA, FitzJohn R, Friendly M, Furneaux B, Hannigan G, Hill MO, Lahti L, McGlinn D, Ouellette MH, Ribeiro Cunha E, Smith T, Stier A, Ter Braak CJF, Weedon J (2024) vegan: Community ecology package (manual).

Olivier JGJ, Bouwman AF, Van Der Hoek KW, Berdowski JJM (1998) Global air emission inventories for anthropogenic sources of NOx, NH3, and N2O in 1990. Environ Pollut 102(Suppl 1):135–148. https://doi.org/10.1016/S0269-7491(98)80026-2

Quast C, Pruesse E, Yilmaz P, Gerken J, Schweer T, Yarza P, Peplies J, Glockner FO (2013) The SILVA ribosomal RNA gene database project: improved data processing and web-based tools. Nucleic Acids Res 41:D590–D596. https://doi.org/10.1093/nar/gks1219

Ray A, Spiro S (2023) DksA, ppGpp, and RegAB regulate nitrate respiration in Paracoccus denitrificans. J Bacteriol 205:e00027–23. https://doi.org/10.1128/jb.00027-23

Remde A, Conrad R (1990) Production of nitric oxide in Nitrosomonas europaea by reduction of nitrite. Arch Microbiol 154:187–191. https://doi.org/10.1007/BF00423331

Remde A, Conrad R (1991) Metabolism of nitric oxide in soil and denitrifying bacteria. FEMS Microbiol Lett 85:81–94. https://doi.org/10.1111/j.1574-6968.1991.tb04700.x

Rinaldo S, Giardina G, Mantoni F, Paone A, Cutruzzolà F (2018) Beyond nitrogen metabolism: Nitric oxide, cyclic-di-GMP and bacterial biofilms. FEMS Microbiol Lett 365:1–9. https://doi.org/10.1093/femsle/fny029

Rognes T, Flouri T, Nichols B, Quince C, Mahé F (2016) VSEARCH: a versatile open source tool for metagenomics. PeerJ 4:e2584. https://doi.org/10.7717/peerj.2584

Romdhane S, Spor A, Aubert J, Bru D, Breuil M-C, Hallin S, Mounier A, Ouadah S, Tsiknia M, Philippot L (2022) Unraveling negative biotic interactions determining soil microbial community assembly and functioning. ISME J 16:296–306. https://doi.org/10.1038/s41396-021-01076-9

Sánchez C, Cabrera JJ, Gates AJ, Bedmar EJ, Richardson DJ, Delgado MJ (2011) Nitric oxide detoxification in the rhizobia-legume symbiosis. Biochem Soc Trans 39:184–188. https://doi.org/10.1042/BST0390184

Skiba U, Fowler D, Smith KA (1997) Nitric oxide emissions from agricultural soils in temperate and tropical climates: Sources, controls and mitigation options. Nutr Cycl Agroecosyst 48:139–153. https://doi.org/10.1023/a:1009734514983

Smith BC, Marletta MA (2012) Mechanisms of S-nitrosothiol formation and selectivity in nitric oxide signaling. Curr Opin Chem Biol 16:498–506. https://doi.org/10.1016/j.cbpa.2012.10.016

Stark JM, Firestone MK (1995) Isotopic labeling of soil nitrate pools using nitrogen-15-nitric oxide gas. Soil Sci Soc Am J 59:844–847. https://doi.org/10.2136/sssaj1995.03615995005900030030x

Subramaniam L, Engelsberger F, Wolf B et al (2024) An innovative soil mesocosm system for studying the effect of soil moisture and background NO on soil surface C and N trace gas fluxes. Biol Fertil Soils 60:1143–1157. https://doi.org/10.1007/s00374-024-01862-5

Vollack KU, Zumft WG (2001) Nitric oxide signaling and transcriptional control of denitrification genes in *Pseudomonas stutzeri*. J Bacteriol 183:2516–2526. https://doi.org/10.1128/JB.183.8.2516-2526.2001

Wendehenne D, Gao Q, Kachroo A, Kachroo P (2014) Free radical-mediated systemic immunity in plants. Curr Opin Plant Biol 20:127–134. https://doi.org/10.1016/j.pbi.2014.05.012

Wink DA, Kasprzak KS, Maragos CM et al (1991) DNA deaminating ability and genotoxicity of nitric oxide and its progenitors. Science 254(5034):1001–1003. https://doi.org/10.1126/science.1948068

Wrage N, Velthof GL, Van Beusichem ML, Oenema O (2001) Role of nitrifier denitrification in the production of nitrous oxide. Soil Biol Biochem 33(12–13):1723–1732. https://doi.org/10.1016/S0038-0717(01)00096-7

Yu M, Lamattina L, Spoel SH, Loake GJ (2014) Nitric oxide function in plant biology: a redox cue in deconvolution. New Phytol 202(4):1142–1156. https://doi.org/10.1111/nph.12739

Zhang J, Kobert K, Flouri T, Stamatakis A (2014) PEAR: a fast and accurate Illumina paired-end read merger. Bioinformatics 30:614–620. https://doi.org/10.1093/bioinformatics/btt593

Zhang T, Liu L, Tan W, Suib SL, Qiu G, Liu F (2018) Photochemical formation and transformation of birnessite: effects of cations on micromorphology and crystal structure. Environ Sci Technol 52(12):6864–6871. https://doi.org/10.1021/acs.est.7b06592